ELSEVIER

Chemical Engineering Journal 80 (2000) 221–231

Chemical Engineering Journal

www.elsevier.com/locate/cej

Pore structure and network analysis of filter cake

C.L. Lin, J.D. Miller*

Department of Metallurgical Engineering, University of Utah, 412 William C. Browning Building, Salt Lake City, UT 84112, USA

Abstract

Filtration is an important solid–liquid separation technology employed widely in the mineral processing industries. The effectiveness of the filtration operation can be influenced by numerous variables, related to the particulate phase, the slurry rheology and the equipment. Continuous filtration of fine particles involves filter cake formation and removal of surface moisture by drawing air through the pore structure network. In order to gain a better understanding of the complex transport phenomena that occur in the filter cake, analysis of the effect of the three-dimensional pore geometry on the effective transport properties of the filter cake is necessary. In this regard, analysis of the pore connectivity in a packed bed of particles should allow for a detailed description of fluid flow and transport in the filter cake structure. Two interrelated approaches, namely computer simulation and experimental measurement, can be used to gain knowledge of pore microstructure and its correlation to macroscopic cake properties. In this regard, a three-dimensional Monte Carlo method was used in this work to simulate cake structure. As the resolution and the techniques for three-dimensional geometric analysis have advanced in the last decade, experimental measurements are now possible to specify in detail the pore structure in three-dimensional digital space using high-resolution X-ray microtomography. Thus in addition to computer simulation, this paper presents preliminary experimental findings of pore structure in three-dimensional using X-ray microtomographic techniques. These experimental results are contrasted to results from computer simulation.

Keywords: Filter cake; Three-dimensional geometric analysis; X-ray microtomography

1. Introduction

Filtration is an important operation employed in mineral processing plants in which slurry is forced through a medium (usually a cloth) in such a way that the particulate phase (filter cake) is retained and liquid passes through the medium [1,2]. Of particular concern in the filtration operation is the capacity and the filter case moisture. Generally, a high filter cake moisture is not desirable because it may affect transportation costs, material handling, and efficiency of subsequent operations [3].

A filter cake can be described as a packed bed of particles with a complex system of interconnected inter-particle voids. The classical approach [1–5] for the analysis of filtration behavior is based on Darcy's law, an empirical equation that describes the one-dimensional fluid flow through a uniform incompressible porous medium and has been used for many years. However, research workers [3,4,6–9] have demonstrated that a filter cake is not of uniform linear character. Normally the porosity is highest at the cake surface and decreases through its depth. The distributions of pore size and shape for filter cakes are usually unknown and difficult to measure.

The physical laws that govern the equilibrium state and the flow of fluids through the filter cake, are simple and well known. In practice, however, only the global physical properties of the system are known at best. Unfortunately, because of the complexity of the pore geometry, it is difficult to predict macroscopic (effective) properties from microscopic (pore level) properties. In this regard, it is essential to develop appropriate experimental techniques and theoretical models to describe in detail the flow which occurs through a packed bed during fine particle filtration. The need for such research efforts is well documented and much attention is being given to this problem as set forth in a recent article published in January 1999 [10].

1.1. Particle packing structure

The knowledge of pore microstructure and its correlation to macroscopic cake properties seems to be an appropriate approach for filtration modeling based on fundamental considerations [11]. Pore structures can be characterized by either experimental observation or computer simulation. Carman [12] commented on research carried out using spheres to simulate packed beds. Other researchers [13–15]

* Corresponding author. Tel.: +1-801-5815160; fax: +1-801-5818119.
E-mail address: jdmiller@mines.utah.edu (J.D. Miller).

1383-5866/00/$ – see front matter
PII: S1383-5866(00)00094-0

studied the effect of size distribution on the packing density. Early methods relying on the microscopic observation of a series of thin sections or polished sections of the porous media (in our case filter cake) were used to characterize the pore microstructure and its interconnected network [9,16–20]. These data sets can then be used to reconstruct and to display the three-dimensional image of the porous system with the help of advanced computer graphic techniques. Complete analysis of the three-dimensional porous structure from serial sections is limited. More recently, techniques have been used, within limits, to obtain direct information about the three-dimensional pore structure [21]. Nuclear magnetic resonance (NMR) imaging instruments map spin densities and relaxation times of hydrogen, and in this way resolves the filling of pore space by fluids. Computerized tomography (CT) is able to show the distribution of solid grains, and pore space filling by liquids or gases. Finally it appears that laser scanning confocal microscopy (LSCM) can precisely image the thin optical planes within thicker porous rock samples. As the resolution and the techniques for three-dimensional geometric analysis have advanced in the last decade, it is now possible to map in detail the pore structure in three-dimensional digital space using high-resolution X-ray microtomography to resolve features with micrometer resolution. A detailed description of the interconnected pore structure based on the concepts of connectivity, percolation, and tortuosity, needs to be developed using three-dimensional X-ray microtomography in order to establish fundamental relationships between complex random pore structures and the corresponding effective transport coefficients.

Mercury intrusion porosimetry has been used to characterize the internal structure of the porous media. Details of how to calculate pore size distributions based on capillary pressure curves obtained from mercury intrusion porosimetry and its limitation can be found in the literature [22]. Recently, more precise information of pore and throat size distributions can be obtained from rate-controlled porosimetry [23].

Computer simulations have been performed in two-dimensional [24,25] and three-dimensional [26–33] in order to obtain and study packing structures. It was observed that the three-dimensional models are more realistic for the simulation of cake structure than the two-dimensional models.

Theoretical models [5,34,35] have been proposed to estimate structural properties and transport phenomena in porous beds. In some cases a reasonable agreement is found between the predicted and calculated parameters. Almost all theory related to transport phenomena in porous media leads to macroscopic laws applicable to systems whose dimensions are large compared with the dimensions of the pores. These macroscopic pore structure parameters represent average behavior of a sample containing many pores. The important macroscopic pore structure parameters important in filtration are porosity, permeability, specific surface area, formation resistivity factor and the breakthrough capillary pressure. A review of the definitions and measurement techniques for these macroscopic parameters is given by Dullien [22]. Generally speaking, the macroscopic quantity of interest is more or less influenced by the microscopic properties of the pore structure and is obtained by a spatial integration of the local field. The overall pore fraction and pore size distribution are two of the most important microscopic parameters which must be used for model development to obtain fundamental relationships between pore structure and the effective transport coefficients. Furthermore, conventional network theory can be used to study the phenomena of flow through a porous structure by treating pores as discrete volumes and connecting these with pore throats as resistances of zero volume. In this regard, network analysis of the three-dimensional connectivity and pore geometry is necessary to determine the effective filter cake transport properties.

1.2. Capillary network model for filter cake

In order to gain a better understanding of the complex transport phenomena that occur in filter cake, a study of the effect of three-dimensional pore geometry on the effective transport properties of the porous media is necessary. Of course, it is known that the agreement will be best if the physical parameters are matched for both model simulation and the actual porous structure. At present, the information from the microscopic pore geometry analysis is not detailed enough to provide an accurate prediction of transport properties for the filter cake from model simulation. Techniques and methodology for a detailed description of the three-dimensional pore structure of a completely interconnected porous system is needed.

Capillary networks, one of the pore structure models, has been used to mimic porous media. For capillary networks, the pore structure is modeled by arrays of capillary tubes. The pore structure of filter cake can be thought to consist of an interconnected three-dimensional network of voids, pores, or capillaries. This three-dimensional network usually has irregular geometry, with different shape and size of capillary segments distributed over the network in irregular fashion. In this regard, it is logical to model capillary pressure curves and other transport properties of filter cake with the help of network models of the pore structure. For example, as shown in Fig. 1, a network model is used to represent the two-dimensional or three-dimensional pore structure of a porous medium. The top left hand side of Fig. 1 shows the two-dimensional view of pores whose intersections, the nodes, are numbered. The symbolic graph of this pore structure can be described in the form of a network of bonds and nodes as shown in the top right hand side of Fig. 1. Capillary network models can be used for the prediction of relative permeability and capillary pressure [18,36].

It is intended to predict the effective transport parameters from microscopic analysis of the three-dimensional interconnected pore structure. To achieve this goal, three major

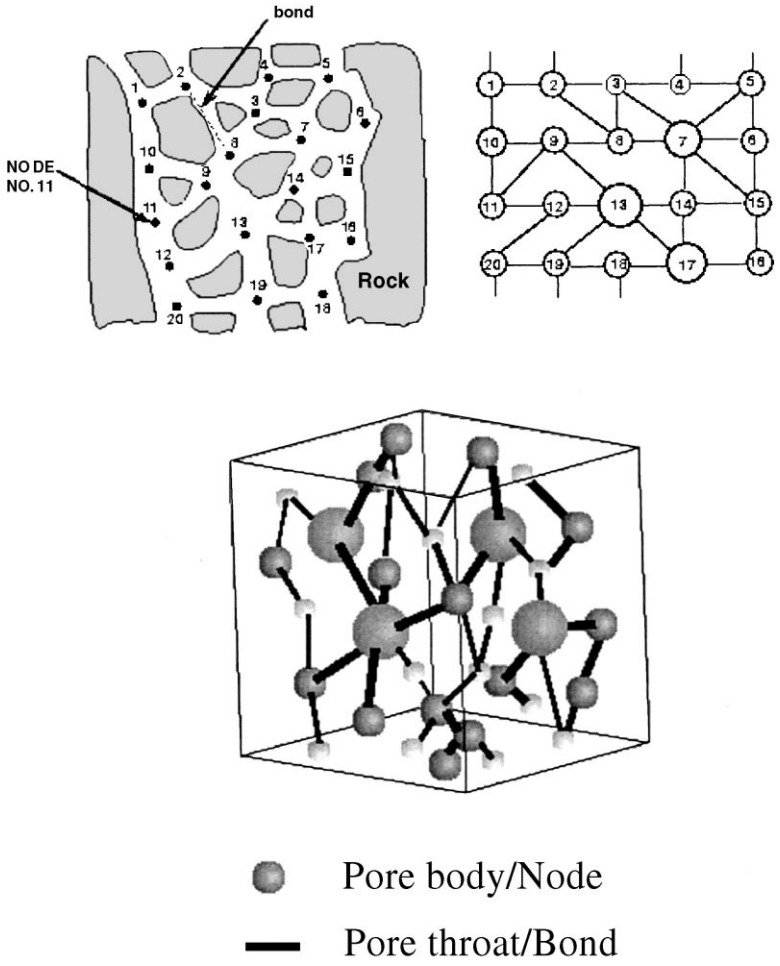

Fig. 1. Symbolic representation of the interconnections in two-dimensional [34] and three-dimensional porous medium.

obstacles need to be overcome. First, a reliable and accurate technique for three-dimensional pore geometry analysis must be established. Second, methodology and procedures for the description of the three-dimensional interconnected pore structure must be established. Finally, based on this description the last task will be to develop the relationship between the effective transport parameters and the microscopic properties of the pore structure. Of course, model verification is an essential step to confirm any simulation work.

Two interrelated approaches, namely computer simulation and experimental measurement, can be used to gain the knowledge of pore microstructure and its correlation to macroscopic cake properties. In this regard, a three-dimensional Monte Carlo method was used in this work to simulate cake formation. Size distributions of two different industrial products whose particle size distributions follow the Rosin–Ramler distribution function were used. The simulated cake structures are described in terms of volume porosity (volume of pore space per unit volume of bed) and surface porosity (area of pore space per unit area of a cross-section). The values of calculated cake porosity for each simulated sample (C and D) were compared with laboratory leaf test data obtained for different products from plant operations. In addition, information on the techniques, methodology, and preliminary experimental findings for network analysis of a completely interconnected porous filter cake is presented using X-ray microtomography.

2. Simulation using Monte Carlo method

Since the particle bed of a filter cake seems to be organized randomly together with some accompanying segregation, a Monte Carlo method should be a useful tool for the simulation of cake structure. A three-dimensional Monte Carlo computer simulation has been done in this work to simulate cake formation. The methodology follows the work of Rosato et al. [25] but in this case the cake structure is achieved in three-dimensional. A random number (r_n) is initially used to generate the center coordinates of each hard spherical particle within a right vertical container. The pair interaction energy $U(s)$ is defined as:

$$U(s) = 0 \quad \text{if} \quad s \geq d_s \tag{1}$$

$$U(s) = \infty \quad \text{if} \quad s < d_s \tag{2}$$

where d_s is the sum of radii of two spherical particles and s is the separation distance between the centers of the two particles.

When simulation starts the particles are created and denoted by:

$$r^* = (r_1, r_2, r_3, \ldots\ldots\ldots, r_n) \tag{3}$$

where r_j is the location (x_j, y_j, z_j) in the coordinate system and j denotes the jth particle.

The total energy of the system $E(r^*)$ can be calculated:

$$E(r^*) = E_g(r^*) + U(s) \tag{4}$$

where $U(s)$ is the pair interaction energy.

$$E_g(r^*) = \text{gravitational potential energy} = \Sigma m_j g z_j \tag{5}$$

where m is the mass of the jth particle and g is the gravitational acceleration.

The Boltzmann distribution gives the probability that a specified configuration having energy $E(r)$ will occur:

$$P[E(r^*)] = 1/n_f \exp[-E(r^*)/k_b T] \tag{6}$$

where n_f is the partition function (normalization constant), k_b is the Boltzmann constant and T is the absolute temperature.

During a cycle, all particles are moved one at a time. The new particle position (trial position) is obtained by the multiplication of a triplet of generated random number (n_x, n_y, n_z) by a small positive number. After each trial, if the total energy decreases ($\Delta E = E_i(r^*) - E(r^*) \leq 0$) the trial is accepted to replace the current configuration. If it does not occur, the probability $P(\Delta E)$ is calculated:

$$P(\Delta E) = P[E_i(r^*)]/P[E(r^*)] = \exp(-\Delta E/k_b T) \tag{7}$$

If the value calculated $P(\Delta E) \geq r_n$, then the new configuration replaces the old one as the current configuration. If $P(\Delta E) < r_n$, the old configuration is kept as the current configuration. The simulation stops when the total energy change is smaller than a pre-defined positive number. Details of the procedure can be found in a previous publication [37].

The three-dimensional filter cake simulation was performed using a computer code which was written in C language and run on a Sun Workstation. The configuration of the environment for simulation was a space with width of 500 μm, length of 500 μm and height of 4000 μm. Initially, the size distribution of two industrial products (pellet feed, Cr and Dr) of Mineracoes Brasileiras Reunidas (MBR), from the iron concentrators of Aguas Claras and Pico (Minas Gerais, Brazil), were considered. The corresponding simulation of these samples are C and D. Table 1 shows, for each sample considered, the size distribution, the number of particles considered for each size interval, the values of α (dispersion constant) and dc (absolute size constant).

Table 1
Size distribution by weight, number of spheres calculated for each size interval, and values of α, and dc, for simulation of samples C and D

Sample	Average size (μm)	Weight%	Number of spheres
C (α=2.18 and dc=57)	111	6.66	11
	63	22.15	201
	48	21.46	440
	41	11.14	367
	34	10.91	630
	26	11.16	1441
	19	7.81	2583
	14	8.71	7201
D (α=1.45 and dc=49)	90	8.92	28
	63	14.78	134
	48	14.21	292
	41	8.32	274
	34	9.32	538
	26	11.60	1499
	19	10.53	3485
	14	22.30	18447

The number of particles was obtained from the weight of particles in each size interval (total weight$\sim 5.0 \times 10^{-4}$ g) using the particle density ($\sim$4.90 g/cm^3) and size.

3. Results and discussion

The porosity values obtained at 10 000 cycles for samples C and D, are 43.11 and 44.09%, respectively. These values represent packing structures usually referred to as random-loose packings [30] and were calculated considering the total space occupied by the particles which was 512 μm in length, 512 μm in width and a final height of cake structure formed. The cake porosity of actual industrial products was roughly estimated from leaf test data using the weight of dry and wet cakes. The results were 54.71% for Cr and 57.29% for Dr. It is evident that the industrial products have a higher porosity than the simulated samples.

The three-dimensional image of the simulated cake and the surface porosity characteristics of the two-dimensional sliced image are shown in Fig. 2. It can be observed, from

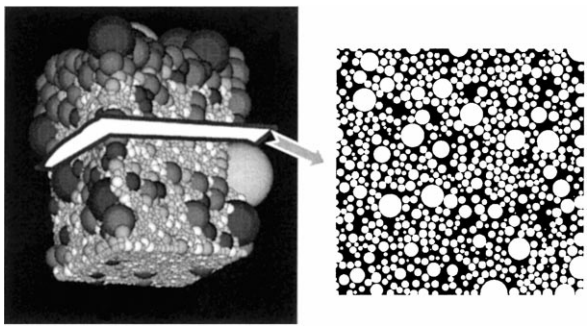

Fig. 2. Three-dimensional images of simulated packed bed for 10 000 cycles and a two-dimensional sectioned image of the particle bed.

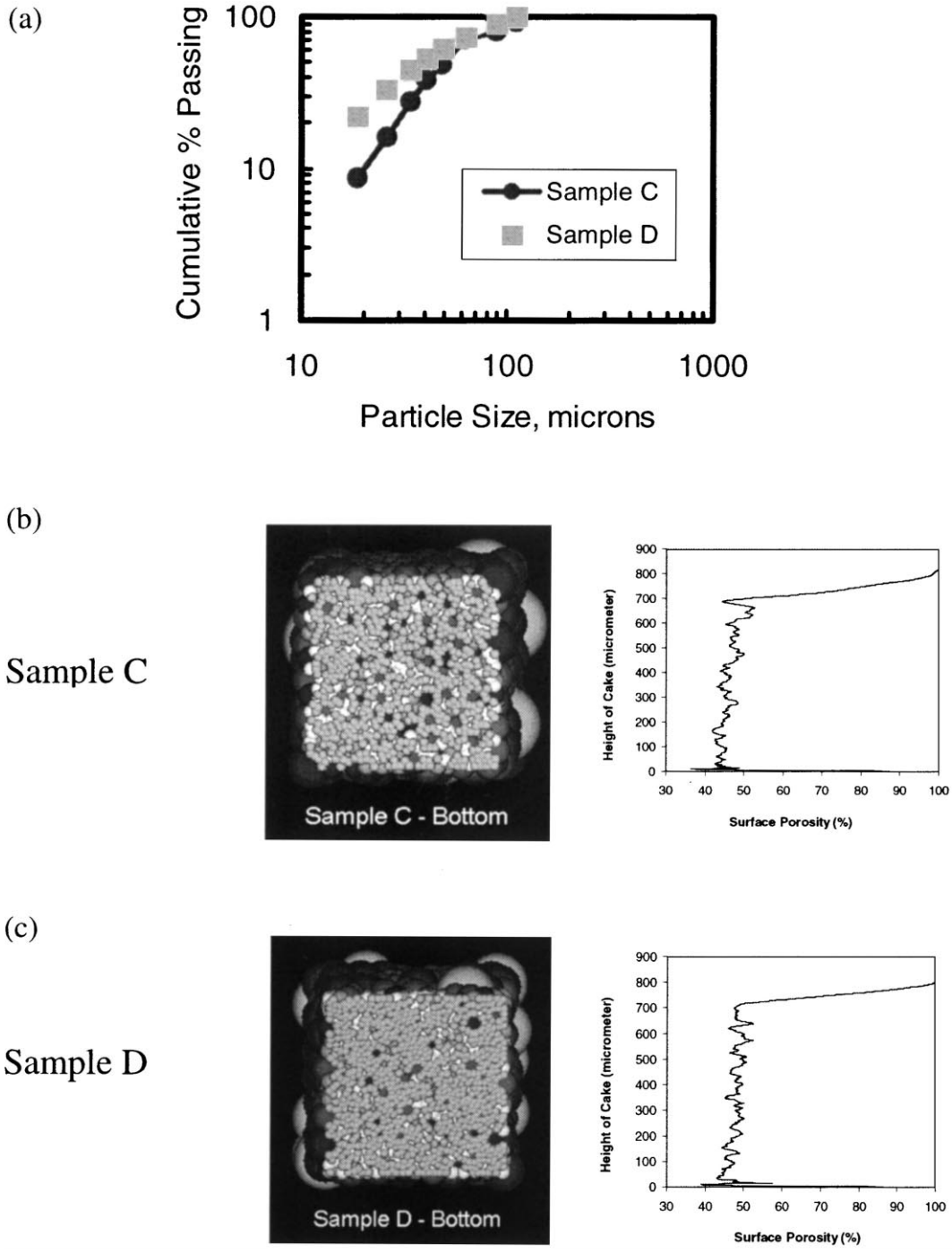

Fig. 3. Comparison of characteristics for samples C and D: (a) particle size distributions; (b) bottom view and height of cake versus surface porosity of sample C; (c) bottom view and height of cake versus surface porosity of sample D.

the three-dimensional images, that the coarse particles tend to reach the top of the cake structure due to segregation. Similar behavior was observed by Rosato et al. [25] for two-dimensional packing structures. Fig. 3(a) shows the size distributions for both samples C and D. The segregation mechanism may be seen more clearly in Fig. 3(b and c) which show images of the bottom view of the simulated cakes through 10 000 cycles for samples C and D, respectively. From the structure of the cake bottom, smaller particles are predominant in sample D and the structures seem to be more closed. Particles from different sizes join the smaller particles and form a more open structure in sample C. It should be noted that the industrial plant and leaf test data establish the filtration performance, which under normal conditions, is higher (i.e. >form filtration rate and <cake moisture) when Cr is used as the filtration feed. Therefore, a

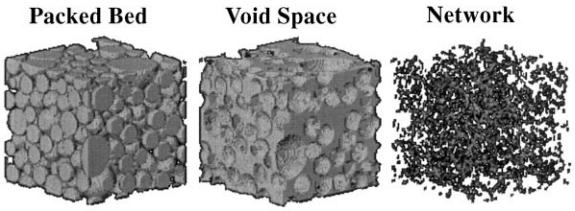

Fig. 4. Network structure of pores in the simulated packed bed of spheres.

preliminary relationship between these cake structures and the filtration behavior is supposed.

Cross-sections, every 1 μm of depth, were done for the simulated cakes and the surface porosity was determined for each section. Comparison of the surface porosity behavior for the simulated cakes is shown in Fig. 3(b and c). Higher values of surface porosity are observed at the top of the cake structure. The variation of the surface porosity with cake depth is similar for both samples. This behavior is in good agreement with the experimental results reported by Van Brakel and Heertjes [14] who used X-ray absorption to determine the variation in surface porosity with depth in the packing structures.

Detailed information regarding the structure of filter cake is an important technological matter since mathematical models will require this information in order to predict and optimize the industrial operations. The simulated cake structures reported in this work will be used subsequently for the analysis of filtration data, and for the development of a structure-based mathematical model. Since the capillary network will be used to mimic the real filter cake, a skeletonization technique should be suitable to build the necessary network and to interpret the linked pore (void) space. Preliminary results of the skeletonization process for the simulated packed bed of spheres is shown in Fig. 4.

3.1. Three-dimensional Pore geometry analysis by X-ray microtomography

The microstructure and the connectivity of the pore space are important to describe fluid flow in filter cake during fine particle filtration. In this regard, characterization of pore structure based on parameters permitting inferences on the fluid balance is of particular interest. The pore structure has to be described by parameters which are of special relevance for the interpretation of fluid transport phenomena. These parameters should be based on directly measured variables of the pore system and not indirect variables (such as those determined empirically from transport processes) valid only for a particular pore structure. In this way fundamental relationships between pore structure and fluid transport at the microstructure level can be described. Thus, it is desired to be able to directly measure the three-dimensional interconnected pore structure of filter cake.

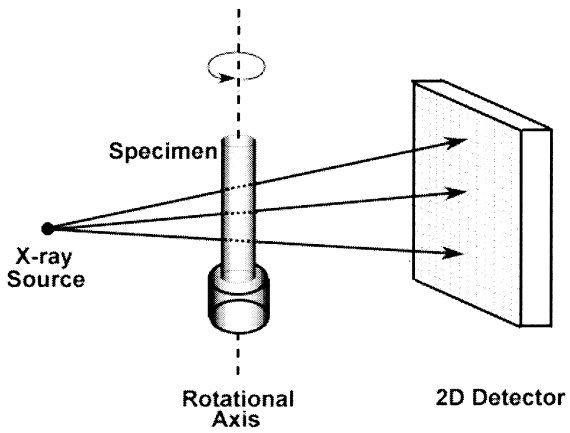

Fig. 5. Schematic diagram of the cone beam X-ray microtomography system.

3.2. High-resolution X-ray microtomography

Cone beam X-ray microtomography [38,39] offers a unique imaging capability which can produce three-dimensional images of the internal structure of samples with micrometer resolution. Rather than rotating the X-ray source and detectors during data collection, as in medical CT technology, the specimen is rotated. Instead of generating a series of two-dimensional sliced images from one-dimensional projections, a three-dimensional reconstruction image array is created directly from two-dimensional projections. Fig. 5 shows a schematic diagram for the cone beam geometry micro-CT system. Details for the description of this micro-CT system and its corresponding reconstruction algorithm can be found in the literature [38].

3.3. Sample preparation

To evaluate the effectiveness of the high-resolution three-dimensional X-ray microtomographic measurement of complex filter cake pore structures, an appropriate specimen was prepared for CT analysis. First, particles, with a size of 210×150 μm in the density range from 2.65 to 5.0 g/cc, were randomly dispersed in epoxy resin, settled to the bottom of a mold and cast into a 7 mm diameter specimen. Then, the specimen was scanned using a cone beam micro-CT at the University of Michigan. Scanning a specimen takes about 20 min. Full three-dimensional reconstruction requires about 2 h. The reconstruction region of this sample is about $7\times7\times7$ mm. The reconstruction set consists of $411\times383\times413$ points or voxels (volume elements). Thus the voxel size is a cube with sides of 17 μm. Fig. 6 illustrates the coordinate system and three slices from different levels of the volume data set for the filter cake specimen.

3.4. Pre-processing three-dimensional cone beam data

The spatial boundary between the pore and the particles can be easily established due to the large difference in

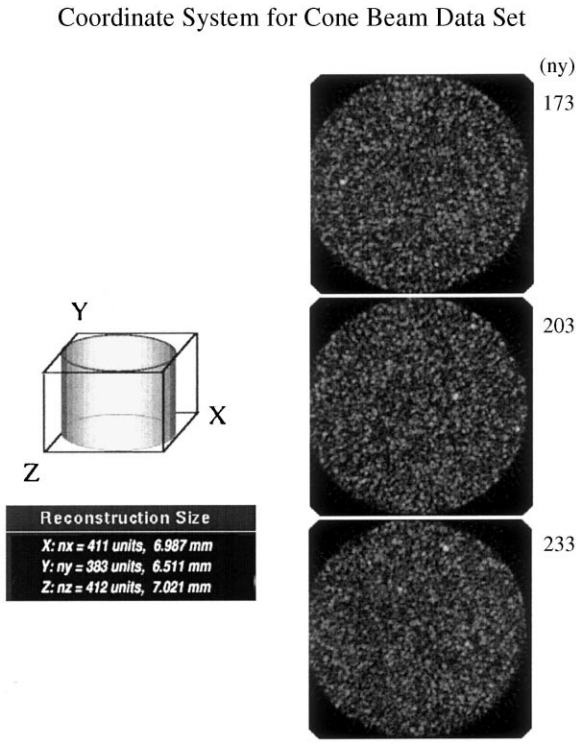

Fig. 6. Coordinate system for the filter cake specimen and selected cross-sectional images.

densities. Threshold techniques can be used to differentiate and classify the original three-dimensional density data in order to have higher quality data. In this regard, the three-dimensional CT data were pre-processed, as shown in Fig. 7, to facilitate the pore geometry analysis. The pre-processing steps are described as follow: (1) cut the three-dimensional digital data set with the size of 256×64×256 from original cone beam data (dimension 411×383×413); (2) threshold the data to obtain binary particle image and (3) invert the data to obtain binary pore image. Fig. 8 shows the schematic diagram for the construction of the volumetric visualization of pore geometry from the original cone beam data set.

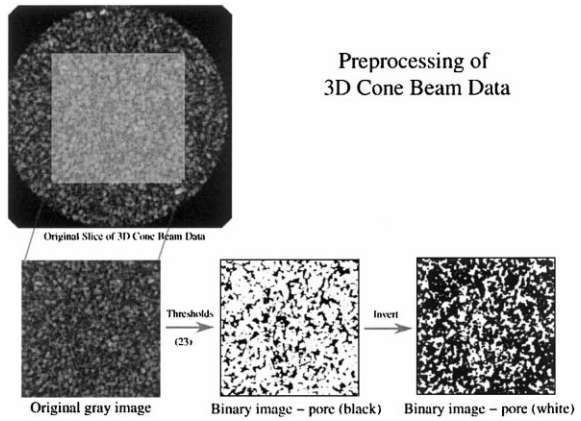

Fig. 7. Pre-processing the cone beam data to extract pore features.

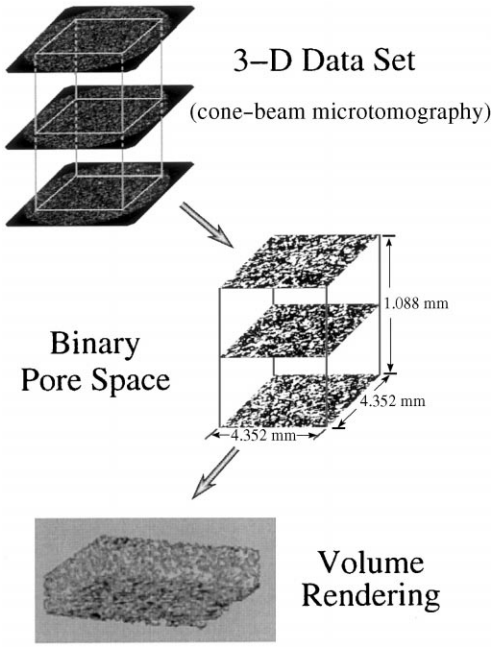

Fig. 8. Schematic diagram for visualization of pore structure from original cone beam three-dimensional data.

3.5. Volumetric image analysis of pore geometry

Most of the techniques available today for digital image analysis are designed for two-dimensional images. Recent advances in computer technology have made the handling of large data sets feasible. Computers with fast computation speeds and sufficient internal memory are required for the processing of three-dimensional data sets. The major difference between the analysis of two- and three-dimensional images concerns the aspect on topology. For instance, in two-dimensional, the algorithm for delineating the object boundary can be easily implemented based on a right-hand-on-wall strategy in which we walk around the object so that the interior always remains to the right until we reach the starting point again. However, in three-dimensional, the boundary is defined by a surface. There is no obvious strategy for tracing a surface. The following sections discuss some of the basic methods for pore geometry analysis of the volumetric filter cake images.

3.6. Porosity, specific surface area, and tortuosity

Porosity, the simplest property of a porous system, is defined as the volume fraction of pores. Specific surface area is defined as the ratio of the surface area of the pores to the bulk volume of the porous medium. The third property, tortuosity, of a porous medium is usually defined as the ratio of the true length of the flow path of a fluid element to the straight-line distance, i.e. the thickness of the filter cake in our case. Based on classical filtration theory, the porosity can be used to predict the permeability defined in Darcy's

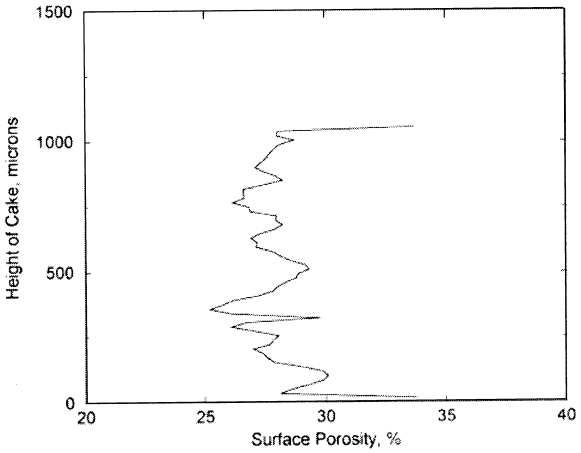

Fig. 9. Surface porosity versus height of filter cake.

law. Porosity, specific surface area and tortuosity of a porous medium, can be used to predict the relative permeability and capillary pressure (given the wettability of the surface) from pore-scale network modelling.

Quantitative information on porosity and specific surface area of a filter cake can be easily determined from the pre-processed binary three-dimensional data set of the complex pore structure. The porosity can be measured as the pore voxel volume (white as shown in Fig. 5) divided by total voxel volume of the three-dimensional data set. The specific surface area can be determined as the total number of pore and particle adjacent voxels divided by the total voxel volume. In our case, the total volume and surface area of pore space were determined as 5.4339 and 190.4512 mm^2, respectively, based on the length of each voxel as 17 μm. The hydraulic radius obtained from the filter cake was 0.02853 mm. The porosity obtained from the filter cake specimen was 27.7%.

Based on the binary three-dimensional data set of pore space, the surface porosity can be determined along the depth of the filter cake. The surface porosity is defined as the ratio between void area and the total area of each cross-section. The surface porosity with respect to the cake depth is shown in Fig. 9. The surface porosity behavior is similar to the results presented from three-dimensional Monte Carlo Simulation and to that reported by Brakel and Heertjes [14].

3.7. Determination of pore body, pore throats and pore size distribution

Although we can directly access the three-dimensional pore structure of the porous media with the use of X-ray microtomography, a fundamental difficulty is how to describe the pore structure. In general, the range of pore sizes is very great in most porous media and the geometric properties of the void system are not easy to define (see Fig. 7). Thus there is a need for the development of an overall concept for the description of the pore structure. In this regard, it is necessary to develop a capillary network from the three-dimensional digital map obtained from X-ray microtomography.

Connectivity is an important concept when flow problems are considered. Fluid flow can occur between two points only when the pore space is connected. The three-dimensional interconnected pore structure is difficult to determine by stacking of two-dimensional thin slices. In addition, to characterize the three-dimensional interconnected pore structure, the term pore size is not easily defined. These open or interconnected pores can not be simply regarded as discrete pseudo-particles. Several two-dimensional image processing techniques can be extended to three-dimensional to characterize the three-dimensional interconnected pore structure and identify features such as pore body or pore throat. The most important algorithms for three-dimensional interconnected pore geometry analysis involve connection of components, erosion, dilation, and skeletonization. Connection of components is critical to determine if a particular feature of pore space is connected or not. Erosion, dilation and skeletonization operations can be used to process and analyze the pore bodies and throats, pore size distribution and interconnected pore structure.

The main concern in volumetric image analysis is the capacity of computer memory. An effective algorithm will be needed such that analysis of the volumetric image can be done sequentially, layer by layer for a huge three-dimensional digital data set. In this regard, a connection-of-components algorithm based on the approach by Hoshen and Kopelman [40] was implemented. Although the binary image of the pore space shown in Fig. 7 is not connected, analysis from three-dimensional connection of components indicates that more than 99% of the pore space belongs to a well connected pore system. Surface rendering of a subset ($64\times64\times64$) of this well connected pore network is shown Fig. 10.

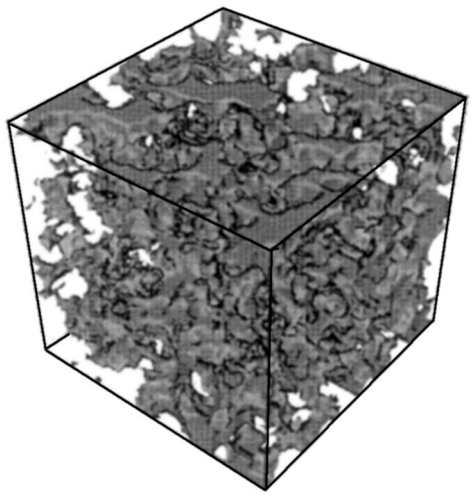

Fig. 10. Surface rendered image of the well connected pore network from subset ($64\times64\times64$) of three-dimensional data set obtained from X-ray microtomography.

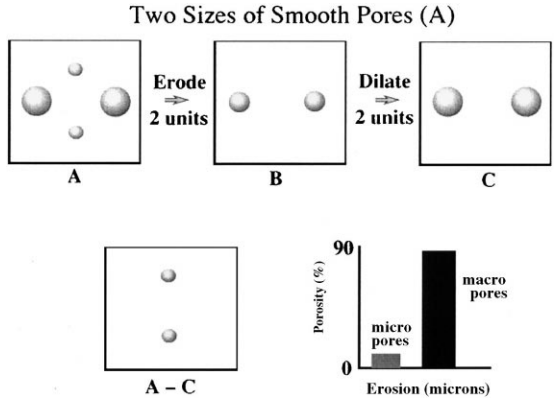

Fig. 11. Schematic representation of pore size measurement using successive erosion/dilation stages.

Pore bodies and throats can be obtained with the use of successive morphological operations, erosion and dilation, as described for two-dimensional [41] and three-dimensional [42] images. Erosions peel away the outer layer of voxels from the three-dimensional pore volumes while dilations replace the outer layer. As shown in Fig. 11, for two different sizes of pores, small pores are completely eliminated after two successive erosions without leaving a seed voxel to restore on subsequent dilation. In this manner, the difference of images A and C (A−C) shows the % loss of pore which is exactly the percentage of micropores (number of erosion or voxel size) in this case. If two pore volumes are connected by a narrow throat, erosion will break the connections and dilation will restore the pore volume but not re-establish the connection, resulting in an increase in the number of pores and a reduction in average pore size as shown in Fig. 12.

Fig. 13 shows three adjacent slices from the three-dimensional cone beam microtomogrphy data for the filter cake specimen converted to a binary image at a voxel intensity threshold level of 23. In this figure the images show the binary porosity (white) following 0, 1, and 2 stages of erosion/dilation (E/D). The small pores or pore throats

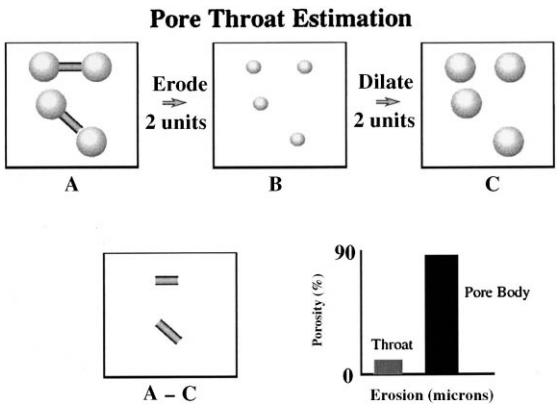

Fig. 12. Schematic representation of estimation of pore body and throat using successive erosion/dilation stages.

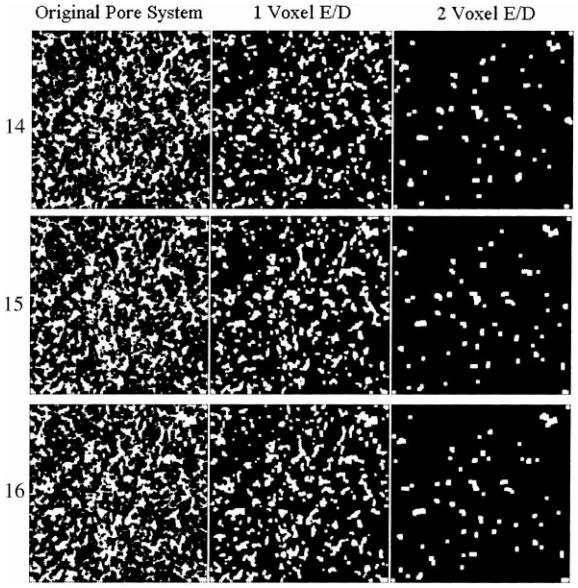

Fig. 13. Three adjacent (14, 15, 16) binary slices of filter cake cone beam microtomographic data at a voxel intensity threshold of 23 following 0, 1 and 2 successive stages of erosion/dilation (E/D).

disappear in successive images with increasing E/D stages until only the large isolated pores remain. Some of these connections which survive the first stage of E/D are shown in the middle column in Fig. 11. In this manner, the largest pore found expressed as a fraction of the total porosity is plotted versus the number of E/D stages [42] as shown in Fig. 14. The original pore structure (no E/D operation) of this filter cake sample has a well-developed pore connectivity. This well connected pore space was found to have more than 99% of the total porosity. After one stage of E/D operation, this sample still exhibits a high degree of connectivity implying that the average pore throats approximate two or more voxel dimensions of 17 μm size per voxel for the filter cake sample. After two stages of E/D much of the pore connectivity has been broken for this sample and the

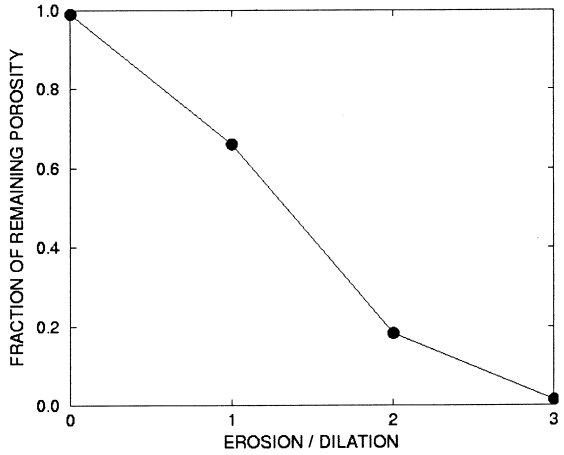

Fig. 14. Fraction of the total porosity remaining after successive stages of E/D for the filter cake sample.

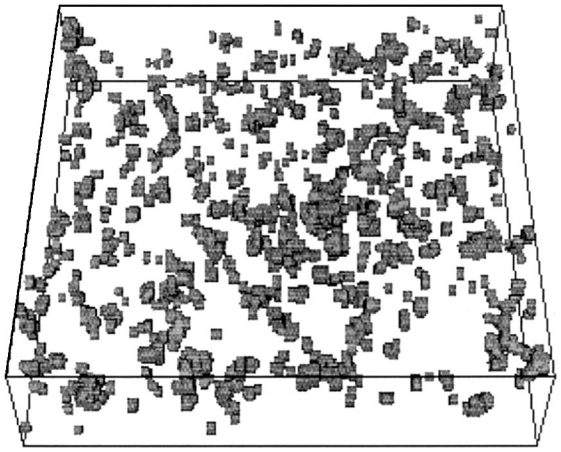

Fig. 15. Three-dimensional view of spatial distribution for isolated pores after two stages of E/D.

results start to approach the isolated pore state shown by the results of Fig. 13. Fig. 15 illustrates the spatial distribution of these isolated pores after two stages of E/D. The pore size distribution based on the equivalent spherical diameter of these isolated pores is shown in Fig. 16.

Since the capillary network will be used to mimic the real filter cake, the skeletonization or medial axis technique [43] should be suitable to build the necessary network and to interpret the linked pore space from the micro-CT three-dimensional digital map. Originally, skeletonization (in a plane) denotes a process which transforms a two-dimensional object into a one-dimensional graph-like structure, comparable to a stick figure. It is thereby essential that the skeleton retains the original connectivity of the shape. Unfortunately, for three-dimensional objects, there are two different types of skeleton: the medial surface and the medial axis. For instance, the medial surface will be generated using a skeletonization process of a slab object. The skeletonization process provides both the radius information and structure of the object space. This information

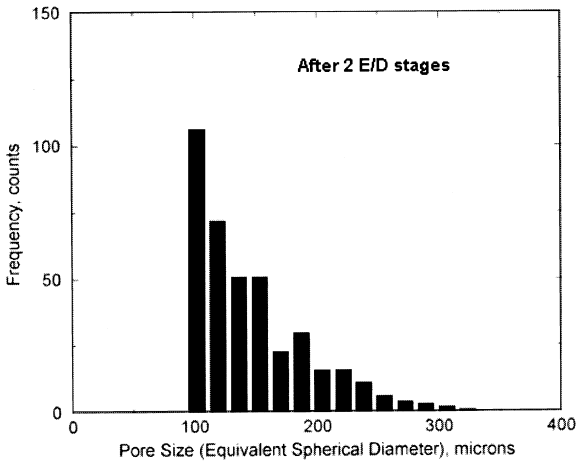

Fig. 16. Pore size distribution after two stages of E/D.

of three-dimensional interconnected pore space provides a tool to describe important properties of the completed pore structure and can be used for the capillary network simulation by percolation theory. Several approaches, topological thinning [44–47], distance transformation (DT) [48,49], discrete Voronoi skeletons (DVS) [50], and marching core method [51] can be used for algorithm development of the three-dimensional skeletonization process. The corresponding length and radius of the skeleton segments from the network graph can be used as attributes of the capillary tubes for the three-dimensional interconnected pore structure. Furthermore, this information can be used to more accurately represent probabilities for the capillary network simulation using percolation theory. Details of the development of three-dimensional skeletonization and percolation theory will be discussed in a separate contribution.

4. Summary

In order to gain a better understanding of the complex transport phenomena that occur in a filter cake, study of the effect of three-dimensional pore geometry on the effective transport properties of the filter cake is necessary. It is possible to simulate a three-dimensional packing, which mimics cake structure, using the Monte Carlo method. The simulated cakes represent what is usually referred to as random-loose packing (ε>42%). The three-dimensional images obtained for simulated samples indicate the significance of segregation during cake formation. The simulated cake bottom structures obtained for samples seem to correlate with laboratory leaf test data obtained for different products from plant operations.

Algorithms for the processing of three-dimensional volumetric images to determine the detailed three-dimensional interconnected pore structure from X-ray microtomography measurements were presented. Pore size measurements on three-dimensional cone beam X-ray microtomogrphic data using successive stages of erosion/dilation has revealed information about the connectivity of the filter cake pore structure and allowed for the estimation of pore throat sizes. Most of the pore throat sizes in this particular sample were found to be less than 34 μm. A skeletonization process should provide for better understanding of the pore structure and allow for the interpretation of the interconnectivity. Finally, the capillary network and percolation process should provide the basis for a predictive model to correlate of transport properties of porous media at various scales. Knowledge of multiphase flow in porous media as will be obtained from such a model should provide important information for practical applications in the design of improved filtration processes.

Acknowledgements

The authors would like to thank the NSF Grant No. CTS-9724315 for the financial support and Dr Robert W.

Goulet and Dr Steven A. Goldstein, University of Michigan, Ann Arbor for performing the CT measurements.

References

[1] D.A. Dahlstrom, C.E. Silverblatt, in: D.B. Purchas (Ed.), Solid Liquid Separation and Scale Up, Uplands, Croydon, 1977, p. 445.
[2] L. Svarosvsky, Filtration Fundamentals, Butterworths, London, 1977.
[3] F.M. Tiller, Solid–Liquid Separation, University of Houston, Houston, 1975.
[4] F.M. Tiller, Filtr. Sep. 12 (1975) 386.
[5] S. Ranjan, R. Hogg, Coal Prep. 17 (1996) 71.
[6] R.M. Kakwani, S.H. Chiang, G.E. Klinzing, Miner. Metall. 1 (1984) 113.
[7] M. Shirato, Filtr. Sep. 9 (1972) 290.
[8] F.S. Bourgeois, G.J. Lyman, Chem. Eng. Sci. 52 (1997) 1151.
[9] F.S. Bourgeois, W.A. Barton, Coal Prep. 19 (1998) 9.
[10] B.O. Paul, Chem. Process. January (1999) 41.
[11] J.D. Miller, C.L. Lin, 13th Annual International Pittsburgh Coal Conference, Proceedings Coal-Energy and the Environment, Pittsburgh, 3–7 September 1996, pp. 826.
[12] P.C. Carman, Trans. Inst. Chem. Eng. 15 (1937) 32.
[13] A.R. Dexter, D.W. Tanner, Nat. Phys. Sci. 238 (1972) 31.
[14] J. Van Brakel, P.M. Heertjes, Powder Technol. 9 (1974) 263.
[15] R.J. Wakeman, Powder Technol. 11 (1975) 297.
[16] J.P. Jernot, et al. J. Microsc. 167 (1992) 9.
[17] W.M. Saltzman, et al. Chem. Eng. Sci. 42 (1987) 1989.
[18] P. Oren et al., Proceedings of the Fifth European Conference on Mathematics of Oil Recovery, Leoben, Austria, September 1996.
[19] C. Lin, M.H. Cohen, J. Appl. Phys. 53 (1982) 4152.
[20] J. Koplik, et al., J. Appl. Phys. 56 (1984) 3127.
[21] L.O. Owen, S.J. Green, Advanced Imaging Techniques for Network Analysis of the Pore Structure of Rocks, Task Report, Terra Tek, Salt Lake City, 1996.
[22] F.A.L. Dullien, Porous Media: Fluid Transport and Pore Structure, 2, Academic, San Diego, CA, 1992.
[23] H.H. Yuan, B.F. Swanson, SPE Form. Eval. 3 (1989) 17.
[24] H.H. Kaush, et al., J. Colloid Interface Sci. 37 (1971) 603.
[25] A. Rosato, et al., Powder Technol. 49 (1986) 59
[26] I. Chatzis, F.A. Dullien, J. Can. Pet. Technol. 16 (1977) 97.
[27] J. Rodriguez, et al., Powder Technol. 47 (1986) 25.
[28] W. Soppe, Powder Technol. 62 (1990) 189.
[29] Y. Konakawa, K. Ishizaki, Powder Technol. 63 (1990) 241.
[30] S.C. Reyes, E. Iglesia, Chem. Eng. Sci. 46 (1991) 1089.
[31] G.T. Nolan, P.E. Kavanagh, Powder Technol. 76 (1993) 309.
[32] C. Hogue, D. Newland, Powder Technol. 78 (1994) 51–56.
[33] K.J. Hwang, et al., Powder Technol. 91 (1997) 105.
[34] N. Ouchlyama, T. Tanaka, Ind. Chem. Fund. 23 (1984) 490.
[35] A.B. Yu, N. Standish, Powder Technol. 52 (1987) 233.
[36] I. Fatt, Trans. AIME Pet. Div. 207 (1956) 144.
[37] Y.K. Yen, et al., Powder Technol. 98 (1998) 1.
[38] L.A. Feldkamp, et al., J. Opt. Soc. 1 (1984) 612.
[39] C.L. Lin, J.D. Miller, Int. J. Miner. Proc. 47 (1996) 61.
[40] J. Hoshen, R. Kopelman, Phys. Rev. B 14 (1976) 3438.
[41] R. Ehrlich, et al. J. Sediment. Petrol. 54 (1984) 1365.
[42] D.A. Doughty, L. Tomutsa, Mag. Reson. Imag. 14 (1996) 869.
[43] H. Blum, Models for the Perception of Speech and Visual Form, MIT, Cambridge, MA, 1967.
[44] Y.F. Tsao, K.S. Fu, Comp. Graph. Image Process. 17 (1981) 315.
[45] W.X. Gong, G. Bertrand, International Conference on Pattern Recognition, 1990, pp. 188.
[46] N. Gagvani, D. Silver, Parameter Controlled Skeletonization of Three Dimensional Objects, Technical Report CAIP_TR_216, Rutgers University, June 1997.
[47] C.M. Ma, M. Sonka, Comp. Vis. Image Underst. 64 (1996) 420.
[48] G. Borgefors, Comp. Vis. Graph. Image Process. 27 (1984) 321
[49] N. Gagvani, D. Silver, Parameter Controlled Skeletonization of Three Dimensional Objects, Technical Report CAIP_TR_216, Rutgers University, June, 1997.
[50] R. Ogniewicz, et al., Proceedings of the Eighth Scandinavian Conference on Image Analysis SCIA '93, Tromso, Norway, 1993, p. 875.
[51] J.D. Furst et al., Proceedings of Mathematical Methods in Biomedical Image Analysis, IEEE Computer Society, San Francisco, CA, June 1996.